CHARACTERIZATION OF MICROSTRUCTURE AND MECHANICAL PROPERTIES OF FSP PROCESSED Al-18Si-0.9Cu-1.15Ni ALLOYS

Abdulmalik, S.S.[1*], Hammajam, A.A.[1] and Feriyanto, D.[2]

[1]Department of Mechanical Engineering, Faculty of Engineering and Technology, Nigerian Army University, P.M.B 1500, Borno State, Nigeria

[2]Department of Mechanical Engineering, Universitas Mercu Buana, Jakarta 11650, Indonisia

*Corresponding email: alhajisani.sa@gmail.com

ASBTRACT

Al-Si alloys produced via casting method consist of cast porosity, coarse eutectic structure, segregation of the large primary Si, and coarse intermetallic particles. The distribution of these particles creates difference in properties along the Al-Si system. During loading it creates different stress field which causes failures in the material. Friction Stir Processing (FSP) is a novel processing technique facilitate by the frictional heat generation between the tool and the workpiece. FSP can triumph over the poor properties due to large sized and unevenly distributed Si particle in the Al matrix. In this investigation, four different process FSP parameters have been used for processing the Al-Si hypereutectic material. Tensile properties, hardness and wear of the friction stir processed material were evaluated and correlated with the microstructure evolution. The characterization of FS-processed material is carried out using optical microscopy (OM), and scanning electron microscopy (SEM). The effect of different tool rotation speeds (800rpm, 1000rpm, 1200rpm, 1400rpm), and fixed traverse speed 22mm/min on microstructural formation, particle size and distribution in the matrix were analyzed and found that the tool speed of 1000rpm resulted in higher tensile 182Mpa, and elongation 7.5%. Higher tool speed 1400rpm could not enhanced the tensile strength further as a result of increasing Si particles, but resulted in increased average microhardness 83.7HV hardness, and wear properties due to dispersion and dissolve intemetallic particles into the stir zone.

Keywords: Alloys, Porosity, Particles, Tensile, Friction, Microscopy

1 INTRODUCTION

Al-Si (hypereutectic) alloys, due to their wide range of advantages such as good castability, high strength, good weldability, wear and corrosion resistance [1], have been used in many applications including automotive engine blocks, cylinders heads, gear boxes, crank case and break cylinder [2]. The microstructure of these alloys especially the hypereutectic series, consist of hard silicon particles distributed in ductile and soft aluminium matrix and hence, it is considered as in situ composite material. Among the drawback of this material is the present of microstructural defects, like; porosities and large coarser silicon particles, which renders the alloy brittle accompanied by low toughness, and strength [3]. Strength of the material could be improved by eliminating porosities and breaking the large silicon particles to smaller smooth particles. Various techniques and approaches such as alloying element addition and heat treatment have been used in order to improve the Al-Si alloy strengths by reducing the microstructural defects and refining the microstructure via changing the silicon particles morphology [4].

Still, those approaches could not effectively changed, redistribute the silicon particle uniformly, and eliminate the porosities [5]. An evolving microstructure modification tool or method; friction stir processing FSP, was used in this study to improve the properties of Al-18Si-0.9Cu-1.15Ni Al-Si alloy. FSP is a variant of friction stir welding FSW, have been reported to modify the microstructure in specific areas especially to enhancing local mechanical properties [2, 6]. During FSP a rotating non-consumable tool having a shoulder and pin is plunged into a piece work material. The tool rubs against the work material and traverses, generates sufficient frictional heat. The heat coupled with intense plastic deformation by the tool pin stirring action and pressure due to the shoulder, result in fine grained, recrystallized microstructure [4]. FSP has been used in Al-Si alloys, shown remarkable improved properties and microstructure refinement [7, 8]. It was reported that FSP effectively eliminates porosities, refines the coarser large primary silicon particles, and eutectic silicon by breaking up and redistributing them into the aluminium matrix [6, 9]. Numerous studies conducted on the influence of FSP were on the properties of hypoeutectic and eutectic Al-Si alloys [4, 7, 9], only limited studies were carried out to evaluate such influence on the properties of hypereutectic Al-Si alloys [5]. Furthermore, in both condition of hypoeutectic and hypereutectic alloy, the influence of FSP on the mechanical properties and microstructure still needs further study, to understand more on the correlation between FSP parameters, tensile, hardness, wear properties and microstructure refinement. Hence, this work is aimed to apply FSP, to modify the surface of Al-18Si-0.9Cu-1.15Ni hypereutectic Al-Si alloy. The effect of tool rotation speeds and traverse speed on microstructure, hardness, wear, and tensile properties and were investigated.

2 METHODOLOGY

The Al-18Si-0.9Cu-1.15Ni material produced by casting method was prepared into plates of size 150mm x 30mm 7mm for friction stir processing. The plates/specimens were rigidly clamped using fixtures in order to avoid misalignment of specimen during processing. Conventional milling machine was used for friction stir processing. Non consumable tool (shoulder diameter 17 mm, pin length 5mm and pin diameter3.5 mm), made from H13 tool-steel was used for experimentation. Initially the tool is allowed to plunge slowly into the material until the shoulder surface touches the workpiece surface. A dwell period of 30 s is maintained to achieve the preheat zone. The tool is traversed at a fixed rate of 22 mm/min to create the defect free processed zone. The FSP treated samples were cut in the transverse direction, ground using grades of sand papers, polished with 0.5μm alumina paste, and etched, using 0.5 M hydrofluoric acid to reveal the microstructures. The as FSP processed samples microstructure examinations was accomplished using scanning electron microscope (SEM). Image analysis technique was utilized for determining the sizes of the silicon particles, intermetallic particles and porosity. To determine the tensile properties, tensile specimens were prepared from the samples (FS-processed regions) along the FSP direction as per ASTM: E8/E8M-11, with the gauge length and gauge width of 25mm and 4mm respectively. The tensile test was carried out using a computer controlled Gotech universal testing machine at 1mm/min cross head speed. Tensile test was done on both the as cast alloy and the FS-processed samples. At every condition, two specimens were tested and their average value was recorded. Fracture surfaces of the tensile specimens were examined using SEM. Samples for microhardness test were grinded and polished. Vickers microhardness was measured across the samples processed zone, using a load of 500 g and dwell time of 10 s. Wear test was conducted using a pin-on-disk tribometer as per G99-04 ASTM standard [10]. Figure 1 shows the schematic representation of the wear test. Rectangular prismatic pins with dimension of 3 mm × 4 mm were prepared from the base alloys and the FS-processed samples. With this geometry it is possible to maintained constant nominal contact area during the wear tests. The counterpart disk was made from AISI steel. The diameter of the sliding track on the disk surface was 82.4 mm. Before the wear test, the surface of each pin was grounded down to 1200 grit abrasive paper. Wear testing was performed in a dry sliding condition for 2000s under a constant load of 20 N and a sliding velocity of 0.5 m/s. All worn-out pins were cleaned in acetone and weighed to an accuracy of ±1 mg prior to testing. Worn surfaces of the wear samples were examined using SEM.

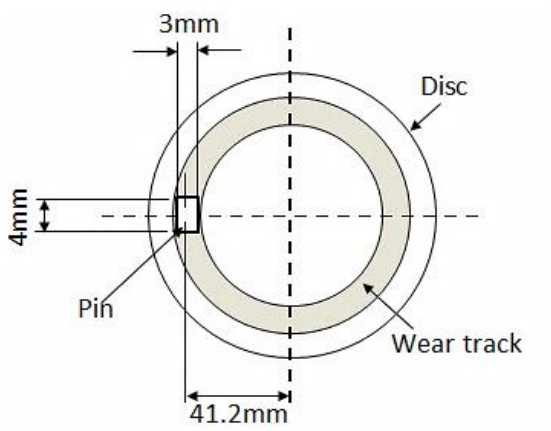

Figure 1. Schematic pin-on-disc wear test

3 RESULTS AND DISCUSSION

Plate 1 shows the SEM micrograph of hypereutectic Al-18Si-0.9Cu-1.15Ni alloy; the halloy consists of coarse needle-like and platelet eutectic, and coarse primary silicon morphology, porosity. And Intermetallic phases such as, AlSiFeNi, and AlSiCuNi, identified via SEM/EDS point analyses. The mean area and the aspect ratio of both the eutectic, primary silicon, and the intermetallic phases measured using image analysis were; 155.1 µm2 with aspect ratio of 2.86), and (123 µm2 and 9) respectively. Moreover, porosity of up to ~94 ECD µm was measured.

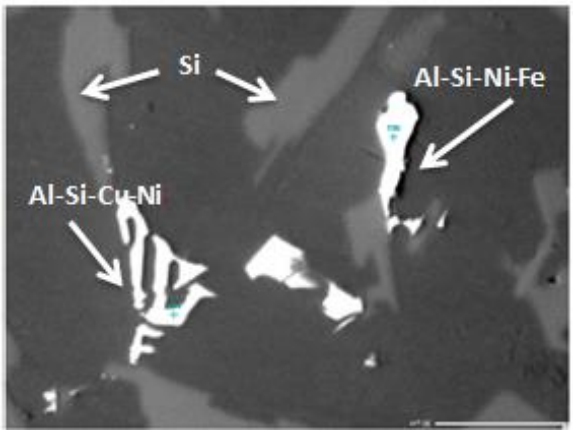

Plate 1. SEM micrograph showing the intermetallic phases in the base alloy

After FSP processing, Plates 2a-d shows micrographs of the processed samples from the center of the stir zones. Quantitative detail of the silicon particles sizes, and aspect ratio, of the as FS-processed Al-18Si-0.9Cu-1Ni samples, relative to tool transverse speeds (22mm/min), and tool rotational speeds (800, 1000, 1200, and 1400 RPM), were recorded in In Table 1. FSP resulted in considerable breaking and reduction of the coarse eutectic and coarse primary silicon particles size and also formed a better distribution of finer and silicon particles in the aluminium matrix. Such microstructure transformation is been reported in other Al-Si alloy [9]. It can be observed, the lowest silicon particles size was achieved at 800rpm rotation speed, implying intense stirring action. But when the tool rotation was increased above 800rpm, it does not result to further decrease. The high heating at higher tool rotation speeds softens the material around the pin. Then, the fragmenting of the particles would not be intensify further, because it became easy for the particles to flow with the plastic flow of the matrix [7].

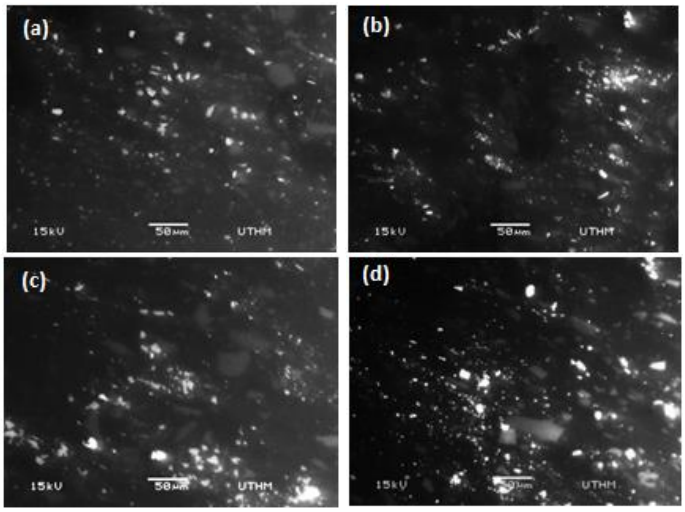

Plate 2. SEM micrograph from the center of stirred zone of Al-18Si-0.9Cu-1Ni alloy after single pass FSP using 22mm/min: (a) 800RPM, (b) 1000RPM, (c) 1200RPM, (d) 1400RPM

Table 1. Quantitative particles sizes, aspect ratio, and porosity

Description	As Cast alloy	800 rpm-22mm/min	1000 rpm-22mm/min	1200 rpm-22mm/min	1400 rpm-22mm/min
Si particles size (μm^2) & aspect ratio	153 / 2.78	49 / 1.7	50.2 / 1.64	62.10 / 1.78	69.56 / 1.89
Intermettalic particles size (μm^2)	121	22.62	21.74	24.42	25.12
Porosity size (ECD)	86	7.24	7.1	7.57	7.8

Changing the rotation speed the particles appears to show some increase in average particle area size and aspect ratio with increased rotation speeds, because when the tool rotation speed increases the frictional heat input during FSP increases which might results into higher than suitable heat and lead to particles increase [5]. This observation agreed with the results presented by [6] who have reported an increase in particle size and aspect ratio with increasing rotation speed. Nevertheless, the average particles sizes achieved in this investigation are very much smaller compare to that of the cast alloy 153μm^2 /2.78 before FSP. Demonstrating that FSP led to about significant reduction in average particle size and shape in terms of mean area values and aspect ratio. From Plate 2a-d, it is clear that all the white eutectic and script shaped intermetallic phases (i.e. AlSiNiFe, and AlSiCuNi), observed in the as cast alloy Figure 1, have been fragmented into smaller sizes and redistributed in the FS-processed samples, showing the influence of tool rotational speeds on morphology, Size and distribution of the intermetallic particles [8]. The decreases of the Al-18Si-0.9Cu-1.15Ni particle size within stir zone is as a result of increased particle fragmentating throughout FSP [11]. This results to a rise in the density of smaller average particles size of Al-18Si-0.9Cu-1.15Ni Table 1. Under each tool rotation speed, the mean area sizes after FSP were considerably smaller than the mean area size of the base material Al(Si,Cu,Ni,Fe) particles 121μm^2. A smaller uniform distribution of intermetallic particles may have some positive effect on both tensile strength and ductility [4]. Earlier studies have demonstrated that on friction stir processing Al-Si eutectic recrystallizes and finer recrystallized grain structure is achieved [2]. Severe plastic deformation and material flow caused by the stirring action of the pin and the high frictional heat to which the material is

exposed during FSP because of the frictional heat are responsible for the grain refinement and dynamic recrystallization present [12]. FSP also results in the closure of casting porosity and a homogenized microstructure [6]. Porosity has been significantly decreased from 94 μm ECD, in the as cast condition to as low as 7.1 ECD after FSP: (7.24 ECD, 7.1 ECD, 7.57 ECD, and 7.8 ECD) for 22mm/min travel speed, and rotational speeds used, due to plastic deformation of the material under the downward force and shear forces of the tool [13]. This trend is consistence with finding of Rao *et al.*, effect of FSP on Al-30Si alloy [3]. It was observed that for all the combination of rotational and traverse tool speeds used in this investigation, FSP induced considerable effect on the microstructure of the base alloy, due to the stirring action of the tool at plastic condition [1]. Silicon particles size variation with changes in rotation is reported for aluminium silicon cast alloys in the course of FSP [6].

3.1 Tensile test

In Table 2, variation of tensile properties and quality index of the base alloy before and after FSP at a varied tool rotational speeds and fixed traverse speed was presented. It is visible to observe that before FSP the mean tensile strength (UTS), of the base alloy: 115 MPa, mean elongation to failure (%El): 1.7 %, and mean (Q): 153 MPa, ware lower compared to all the FS-processed samples. That was largely because of the presence of porosities and larger brittle silicon particles, presence in the alloy and acted as crack initiation sites [14]. After FSP, the FS-processed samples showed significant increases in tensile properties. The UTS is improved up to 29%, and ductility of 4.4%, largely due to the refinement of the microstructure and the reduction/elimination of porosities. Other studies also have found that the tensile properties and fatigue of cast aluminium silicon alloys improved with refined microstructure, and reducing casting defect such as porosities size and density [15]. In addition, a more better distribution of intermetallic particles may have some effect on both tensile strength, and ductility, as reported by [4].

Table 2. Tensile properties and quality index

Description	Q (MPa)	UTS (MPa)	%El
As cast alloy	153	115	1.7
800rpm- 22mm/min	297	179	6.1
1000 rpm-22mm/min	312	182	7.5
1200 rpm-22mm/min	287	173	5.8
1400 rpm-22mm/min	263	155	5.3

Sample processed at 1000rpm shows higher tensile strength and elongation 182MPa / 7.5% compared with the other samples. The higher tensile strength, elongation obtain at the 1000rpm is related to the uniform distribution of small, fine Si particles in the aluminium matrix of the stir zone Plate 2, whereas the reduction of the strength at 1200rpm (173MPa /5.8%) to 1400rpm (155MPa / 5.3%) was due to the increased primary and eutectic Si particles in the matrix [16]. At 1000rpm-22mm/min, the sample tensile properties Table 2, raise through the maximum which mean at that condition there was sufficient stirring and proper consolidation of material and plasticization [17]. But as the tool speed increase to 1400rpm the properties decrease and that maybe due to coarsening of particles at more than sufficient heat because of increased tool speed. A significant heat rise leads to particles coarsening, this in turn can cause a decrease in strength [2]. The effect of the FSP on the performance of the Al-18Si-0.9Cu-Ni alloy was also evaluated using a numerical index that depends on the metallurgical qualities of the alloy: quality index (Q) [13]. Rather than tensile and elongation alone, the quality index combines the strength and ductility and presents a description of the true tensile properties of the cast material and samples [18]. The as cast alloy quality index, was increased to 297MPa, 312MPa, 287MPa, 263MPa, at 22mm/min traverse speed. This is due to porosity elimination as well as refinement of grains and intermetallic particles [13]. Plate 3, presents the fracture surfaces for the unprocessed base alloy and the as FS-processed tensile samples examined using

SEM to determine their resulted failure pattern. Figure 1.3a shows the as cast alloy tensile sample fracture surface. It can be seen that the surface was dominated by cleavage planes which indicate a brittle failure pattern; results in lower ductility. The cleavage pattern in fracture surface gives the indication of brittle material [19]. The FS-processed samples shows fracture surface with dimple rupture pattern Plate 3b-e. Formation of dimple pattern generally gives the indication of ductile material [8]. When these FSP samples were subjected to tensile testing the micro voids nucleated after certain level of straining, but interlinking of these micro cracks became difficult and therefore allowed the ligament to deform considerably; resulted in high ductility. The nucleation of micro voids at the particle matrix interface represents dimple like pattern in the fracture surface [8], which is evident in Plate .3b-e.

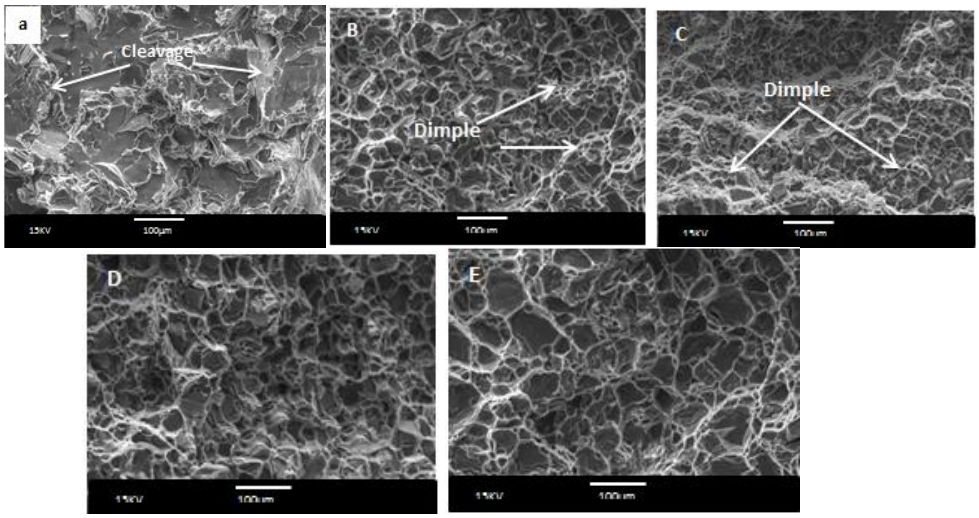

Plate 3. Fracture surfaces; (a) cast base alloy, and as FS-processed tensile samples using 22mm/min: (b) 800RPM, (c) 1000RPM, (d) 1200RPM, (e) 1400RPM

3.2 Microhardness

The as-cast alloy displayed average hardness values 63.7HV. Figure 1.4, Presents the average hardness of the stirred zone measured after FSP; the processed samples relative to the rotation speeds, shows increasing trend in the average hardness from 3% up to about 20% for the higher tool rotational speed. This can be ascribed to differences in microstructural alterations through the processed zone during FSP [12]. As shown Figure 2 at the higher tool speed sample, the higher values of hardness obtained may be ascribed to the fact that that sample possess better combinations of the modified Si structure and a considerable dispersion of the Ni-rich precipitation-hardening phases, Plate 2. The enhanced hardness values obtained at the high heat input samples are regulated by the greater dispersion of the intermetallic phase precipitated in samples, as well as the considerable degree of modification induced by the intermetallic particles [20]. This is due to the fact that the hardening effect caused by the intermetallic phase is greater than the softening effect resulting from a lower coarsening rate of Si particles [21]. Thus, the hardening effect caused by the Ni-rich phase is a factor of greater significance than the softening effect due to modification. This maybe the reason for which the samples exhibit increased hardness values as the tool speeds increases. In Figure 2 the mean hardness was found increasing with raising the tool spindle rate [22]. Similarly, [7] found that the hardness increases by raising tool rotational rate. And have concluded that the reason for increased hardness was due to refinement, and distribution of fine Si particles as well as dispersion of intermetallic particles at higher tool speeds [4].

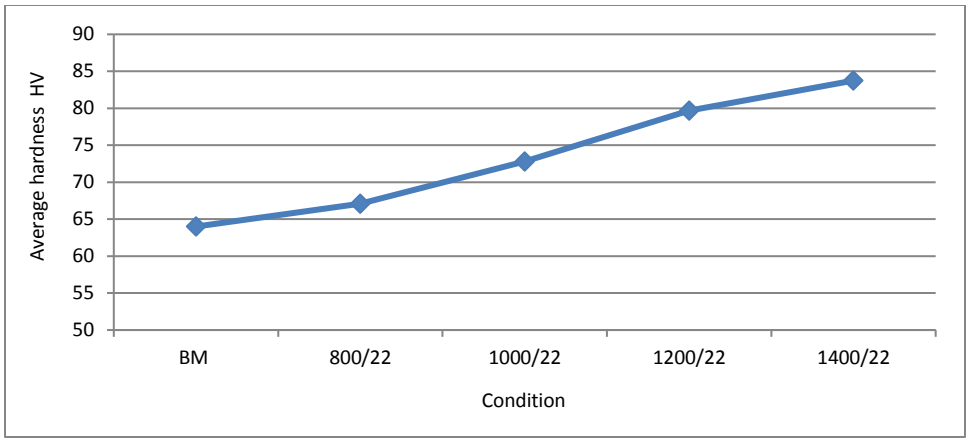

Figure 2. Showing variation of mean hardness within the processed zone relative to tool rotation speed and traverse speed.

3.3 Wear test

Plate 4 compares the wear surfaces of the as cast base alloy and the FS-processed samples. For the as cast base alloy the worn surface morphology consists of a combination of adhesion regions, and delamination areas. Also, craters can be seen on the worn surfaces as indicated by arrows in Plate 4a. The presence of the craters in the worn surface can be explained by the leakage of hard Si particles during the sliding process and due to the detachment of wear debris [23]. The surface of the sample experiences a large plastic deformation due to the surface traction during sliding [7]. Plate 4(b)-(e) shows SEM micrographs of the worn surfaces of FS-processed samples. It shows scratched grooves, small craters, and less delamination, are the main features on the surfaces. It is clear that the worn surface of the FS-processed samples appeared less damaged than the worn surface of the as-cast sample [24]. These features imply ductile wear as the predominant wear mode [25]. Wear surface of the samples in Plate 4(e) condition shows less surface damage. This difference in wear damage indicates mainly abrasive and less delamination wear account for the features observed in these samples [26] It also accounts for the improvement in wear resistance of the samples [24]. This improvement in wear resistance may be due to the enhanced hardness in these FS-processed samples. An increase in hardness leads to reduction in the adhesion and delamination of the sample [26], in turn decreasing the formation of asperities junction, resulting in the lower surface damage of the sample [27]. From Figure 2, the microhardness of FSP samples within the SZ higher than that of base metal specimen can be achieved. Since the indentation hardness can help to predict wear rate in the Al-Si series alloy system [28], the increased hardness resulted from the refined microstructures, as shown in Plate 2, can help to improve the wear resistance for FS-processed conditions. In other words, the improvement of the wear resistance should be mainly due to the modification of eutectic/primary Si and Ni-rich intermetallic in the SZ. The surface damage of the FS-processed samples decreases as the tool rotation speed increases, this is related with enhancement in hardness due to microstructure refinement. Unlike unmodified coarse second phase particles Plate 2 which can be subjected to significant brittle fracture, refined particles are more resistant to the impingement. The plowing craters and cracks can significantly be impeded by these residual Si and Ni intermetallic particles. The uniformly dispersed fine particles, which can still remain on the wear surface of FS-processed samples, are eutectic Si and Ni intermetallic particles. This result, which suggests uniformly, dispersed fine Si and Ni-rich intermetallic particles as the major strengthening phases to increase the wear resistance to FS-processed.

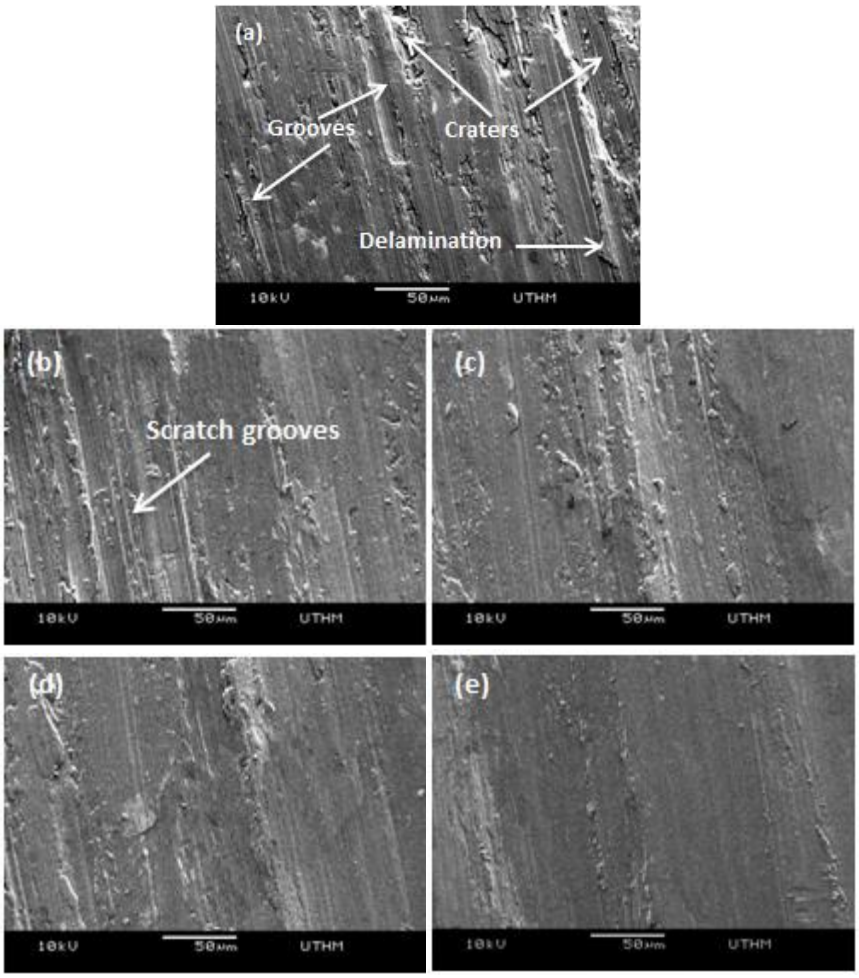

Plate 4. Worn surfaces of (a) the as cast base metal, and FS-processed tensile samples using 22mm/min: (b) 800RPM, (c) 1000RPM, (d) 1200RPM, (e) 1400RPM

4 CONCLUSIONS

At the end of this study the following conclusions can be derived. Of the four varied process parameters used in the friction stir process of Al-18Si-0.9Cu-1.15Ni samples, the 1000rpm-22mm/min was identified as the better process parameter in which the sample under this condition yielded highly refined macrostructure in FSP region and yielded a maximum tensile strength of 182 MPa and percentage elongation of 7.5%. While the sample processed under 1400rpm-22mm/min condition yielded the highest average microhardness of 83.7 HV, and less damaged wear surface. Presence of very fine recrystallized microstructure, breakups of Si particles to fine and smaller size, enhance distribution of intermetallic particle in the samples stir zone enabled by the frictional heat generation through the tool shoulder contact, and stirring action by the tool pin are the reasons for enhanced tensile properties, microhardness, and wear of the processed zone/sample.

REFERENCES

1. Jayaraman, M., Sivasubramanian, R. and Balasubramanian, V. (2009). Effect of process parameters on tensile strength of friction stir welded cast LM6 aluminium alloy joints. *Journal of Materials Science & Technology*, vol. 25, no. 5, pp. 655-664.

2. Karthikeyan, L., Senthilkumar, V. and Padmanabhan, K. (2010). On the role of process variables in the friction stir processing of cast aluminum A319 alloy. *Materials & Design*, vol. 31, no. 2, pp. 761-771.

3. Rao, A.G., Deshmukh, V.P., Prabhu, N. and Kashyap, B.P. (2016). Enhancing the machinability of hypereutectic Al-30Si alloy by friction stir processing. *Journal of Manufacturing Processes*, vol. 23, pp. 130-134.

4. Tsai, F. and Kao, P. (2012). Improvement of mechanical properties of a cast Al–Si base alloy by friction stir processing. *Materials Letters*, vol. 80, pp. 40-42.

5. Mahmoud, T. (2013). Surface modification of A390 hypereutectic Al–Si cast alloys using friction stir processing. *Surface and Coatings Technology*, vol. 228, pp. 209-220.

6. Mahmoud, T. and Mohamed, S. (2012). Improvement of microstructural, mechanical and tribological characteristics of A413 cast Al alloys using friction stir processing. *Materials Science and Engineering: A*, vol. 558, pp. 502-509.

7. Alidokht, S.A., Abdollah-zadeh, A., Soleymani, S., Saeid, T. and Assadi, H. (2012). Evaluation of microstructure and wear behavior of friction stir processed cast aluminum alloy. *Materials Characterization*, vol. 63, pp. 90-97.

8. Guru, P., Panigrahi, S. and Ram, G.J. (2015). Enhancing strength, ductility and machinability of a Al–Si cast alloy by friction stir processing. *Journal of Manufacturing Processes*, vol. 18, pp. 67-74.

9. Aktarer, S.M., Sekban, D.M., Saray, O., Kucukomeroglu, T., Ma, Z.Y. and Purcek, G. (2015). Effect of two-pass friction stir processing on the microstructure and mechanical properties of as-cast binary Al–12Si alloy. *Materials Science and Engineering: A*, vol. 636, pp. 311-319.

10. Shafiei-Zarghani, A., Kashani-Bozorg, S. and Zarei-Hanzaki, A. (2011). Wear assessment of Al/Al 2 O 3 nano-composite surface layer produced using friction stir processing. *Wear*, vol. 270, no. 5, pp. 403-412.

11. Pasebani, S., Charit, I. and Mishra, R.S. (2015). Effect of tool rotation rate on constituent particles in a friction stir processed 2024Al alloy. *Materials Letters*, vol. 160, pp. 64-67.

12. Karthikeyan, L., Senthilkumar, V.S., Balasubramanian, V. and Natarajan, S. (2009). Mechanical property and microstructural changes during friction stir processing of cast aluminum 2285 alloy. *Materials & Design*, vol. 30, no. 6, pp. 2237-2242.

13. Sun, N. and Apelian, D. (2013). Localized microstructure enhancement via Friction Stir Processing for die cast components. *La Metallurgia Italiana*, vol. 10, pp. 3-13.

14. Chan, C.Y. (2011). Friction Stir Processing of Aluminium-Silicon Alloys. *University of Manchester*,

15. Vijayavel, P., Balasubramanian, V. and Sundaram, S. (2014). Effect of shoulder diameter to pin diameter (D/d) ratio on tensile strength and ductility of friction stir processed LM25AA-5% SiCp metal matrix composites. *Materials & Design*, vol. 57, pp. 1-9.

16. Tajiri, A., Uematsu, Y., Kakiuchi, T., Tozaki, Y., Suzuki, Y. and Afrinaldi, A. (2015). Effect of friction stir processing conditions on fatigue behavior and texture development in A356-T6 cast aluminum alloy. *International Journal of Fatigue*, vol. 80, pp. 192-202.

17. Gandra, J. (2014). Friction stir processing. *Surface Modification by Solid State Processing*, pp. 73-111.

18. Ahmad, R. and Asmael, M. (2016). Influence of Lanthanum on Solidification, Microstructure, and Mechanical Properties of Eutectic Al-Si Piston Alloy. *Journal of Materials Engineering and Performance*, pp. 1-15.

19. Rao, A.G., Deshmukh, V.P., Prabhu, N. and Kashyap, B.P. (2015). Ductilizing of a brittle as-cast hypereutectic Al–Si alloy by friction stir processing. *Materials Letters*, vol. 159, pp. 417-419.

20. Mousavi, G., Emamy, M. and Rassizadehghani, J. (2012). The effect of mischmetal and heat treatment on the microstructure and tensile properties of A357 Al–Si casting alloy. *Materials Science and Engineering: A*, vol. 556, pp. 573-581.

21. El Sebaie, O., Samuel, A.M., Samuel, F.H. and Doty, H.W. (2008). The effects of mischmetal, cooling rate and heat treatment on the eutectic Si particle characteristics of A319. 1, A356. 2 and A413. 1 Al–Si casting alloys. *Materials Science and Engineering: A*, vol. 480, no. 1, pp. 342-355.

22. El-Danaf, E.A. and El-Rayes, M.M. (2013). Microstructure and mechanical properties of friction stir welded 6082 AA in as welded and post weld heat treated conditions. *Materials & Design*, vol. 46, pp. 561-572.

23. El Aal, M.I.A. and Kim, H.S. (2014). Wear properties of high-pressure torsion processed ultrafine grained Al–7% Si alloy. *Materials & Design*, vol. 53, pp. 373-382.

24. Soleymani, S., Abdollah-zadeh, A. and Alidokht, S.A. (2011). Improvement in tribological properties of surface layer of an Al alloy by friction stir processing. Journal of Surface Engineered Materials and Advanced Technology, vol. 1, no. 3, pp. 95-100.

25. Alidokht, S.A., Abdollah-zadeh, A., Soleymani, S. and Assadi, H. (2011). Microstructure and tribological performance of an aluminium alloy-based hybrid composite produced by friction stir processing. *Materials & Design*, vol. 32, no. 5, pp. 2727-2733.

26. Van Thuong, N., Zuhailawati, H., Abu Seman, A., Huy, T.D. and Dhindaw, B.K. (2015). Microstructural evolution and wear characteristics of equal channel angular pressing processed semi-solid-cast hypoeutectic aluminum alloys. *Materials & Design*, vol. 67, pp. 448-456.

27. Chen, Y. and Nakata, K. (2009). Evaluation of microstructure and mechanical properties in friction stir processed SKD61 tool steel. *Materials characterization*, vol. 60, no. 12, pp. 1471-1475.

28. Yii, S.J., Norazman, A., Nasir, R.M. and Anasyida, A.S. (2016). Microstructural and mechanical properties of Al-20% Si containing cerium. *Procedia Chemistry*, vol. 19, pp. 304-310.